Inorg. Chem. **2006**, *45*, 3415–3423

Oxidation of Iodide by a Series of Fe(III) Complexes in Acetonitrile

Xiaoguang Wang and David M. Stanbury*

Department of Chemistry, Auburn University, Auburn, Alabama 36849

Received November 23, 2005

The oxidations of iodide by $[Fe^{III}(bpy)_2(CN)_2]NO_3$, $[Fe^{III}(dmbpy)_2(CN)_2]NO_3$, $[Fe^{III}(CH_3Cp)_2]PF_6$, and $[Fe^{III}(5\text{-Cl-phen})_2(CN)_2]NO_3$ at 25 °C, ionic strength of 0.10 M in acetonitrile, are catalyzed by trace levels of copper ions. This copper catalysis can be effectively masked with the addition of 5.0 mM 2,2′-bipyridine (bpy), which permits the rate law of the direct reactions to be determined: $-d[Fe(III)]/dt = 2(k_1[I^-] + k_2[I^-]^2)[Fe(III)]$. According to ^1H NMR and UV–vis spectra, the products of the reaction are I_3^- and the corresponding Fe(II) complexes, with the stoichiometric ratio ($\Delta[I_3^-]/\Delta[Fe(II)]$) of 1:2. Linear free-energy relationships (LFERs) are obtained for both log k_1 and log k_2 vs $E_{1/2}$ with slopes of 16.1 and 13.3 V^{-1}, respectively. A mechanism is inferred in which k_1 corresponds to simple electron transfer to form $I^\bullet$ plus Fe(II), while k_2 leads directly to $I_2^{-\bullet}$. From the mild kinetic inhibition of the k_1 path by $[Fe^{II}(bpy)_2(CN)_2]$ the standard potential (E°) of $I^\bullet/I^-$ is derived: $E^\circ = 0.60 \pm 0.01$ V (vs $[Fe(Cp)_2]^{+/0}$).

Introduction

The redox chemistry of iodide in water is quite well understood, but this chemistry is considerably less developed in other solvents. For example, there are no reports of rate laws of reactions with typical outer-sphere oxidants in pure dipolar aprotic solvents such as acetonitrile, although there are dozens of reactions with published rate laws for such oxidants in aqueous media. Our initial effort to redress this imbalance revealed an unanticipated complication: trace levels of copper ions are potent catalysts for the oxidation of iodide by $[Fe^{III}(bpy)_2(CN)_2]^+$ in acetonitrile (bpy = 2,2′-bipyridine).[1] Such catalysis is unknown for outer-sphere iodide oxidations in aqueous media, with the possible exception of the reaction of $[Fe(CN)_6]^{3-}$.[2]

Another notable difference between iodide in acetonitrile and in water is in its voltammetric response. In water iodide displays a single oxidation wave, while two waves are seen in acetonitrile.[3] The first wave in acetonitrile is due to the net oxidation of iodide to I_3^-, and the second wave is due to the oxidation of I_3^- to I_2. The separation between the two waves is related to the equilibrium constant for the association of I^- with I_2, for which the pK is −9.8 in acetonitrile.[4] This association constant is much smaller in aqueous solution, which leads to an overlap of the two waves.

Iodine atoms and $I_2^{-\bullet}$ are prominent intermediates in the mechanisms proposed for outer-sphere oxidation of iodide in aqueous media.[5] These two radicals would be anticipated intermediates in outer-sphere iodide oxidations in acetonitrile, providing that the complications arising from trace copper catalysis could be surmounted. Iodine atoms in acetonitrile can be generated by photolysis of I^-, and their UV spectrum has been recorded.[6] $I_2^{-\bullet}$ in acetonitrile is produced during photolysis of I^- through the association of $I^\bullet$ with I^- [6] and also in the photolysis of I_3^-;[7] this species has a characteristic absorption feature around 390 nm. Efforts to determine the equilibrium constant for association of $I^\bullet$ with I^- have not been fully successful because the reaction is so strongly driven and only a lower limit could be specified for the equilibrium constant.[6] $I^\bullet$ and $I_2^{-\bullet}$ have standard potentials that are quite accurately determined in aqueous solution,[8] but there is no report on the corresponding quantities in acetonitrile save for the flawed estimate (vs "NHE") from Eberson.[9,10]

Current interest in the redox chemistry of iodide in acetonitrile is stimulated by the development of dye-sensitized photoelectrochemical cells ("Grätzel cells") that typically depend on the oxidation of iodide in a dipolar

* To whom correspondence should be addressed. E-mail: stanbdm@auburn.edu.

(1) Wang, X.; Stanbury, D. M. *J. Phys. Chem. A* **2004**, *108*, 7637−7638.
(2) Kimura, M.; Shiota, Y.; Kishi, S.; Tsukahara, K. *Bull. Chem. Soc. Jpn.* **1999**, *72*, 1293−1299.
(3) Popov, A. I.; Geske, D. H. *J. Am. Chem. Soc.* **1958**, *80*, 1340−1352.
(4) Baucke, F. G. K.; Bertram, R.; Cruse, K. *J. Electroanal. Chem.* **1971**, *32*, 247−256.
(5) Nord, G. *Comments Inorg. Chem.* **1992**, *13*, 221−239.
(6) Treinin, A.; Hayon, E. *Int. J. Radiat. Phys. Chem.* **1975**, *7*, 387−393.
(7) Walhout, P. K.; Alfano, J. C.; Thakur, K. A. M.; Barbara, P. F. *J. Phys. Chem.* **1995**, *99*, 7568−7580.
(8) Stanbury, D. M. *Adv. Inorg. Chem.* **1989**, *33*, 69−138.

10.1021/ic052022y CCC: $33.50
Published on Web 03/24/2006

aprotic solvent and where the oxidant is a derivative of $[Ru^{III}(bpy)_2(SCN)_2]^+$.[11−14] Study of this specific oxidant, however, is hampered by its instability in solution.[15] Related oxidants such as $[Fe^{III}(bpy)_2(CN)_2]^+$ are much more convenient to study in solution, and they have been shown to be highly effective as sensitizers in photoelectrochemical cells of the Grätzel type.[16−18]

The present paper reports on the kinetics and mechanism of oxidation of I^- in acetonitrile by $[Fe^{III}(bpy)_2(CN)_2]^+$ and several other singly charged Fe(III) oxidants. Catalysis by trace levels of copper ions is demonstrated to be a general phenomenon and not dependent on the presence of potentially bridging ligands such as CN^-. By use of an effective Cu-ion scavenger, the rate law and stoichiometry of the direct oxidation of I^- are determined. The LFERs are developed for the rate constants, which should be helpful in estimating rate constants for oxidation of I^- by other oxidants. A mechanism is inferred that features $I^\bullet$ and $I_2^{-\bullet}$ as intermediates, and an evaluation of $E°$ for the $I^\bullet/I^-$ redox couple is derived from the kinetic effects of Fe(II).

Some comments regarding the use of redox potentials in this paper are necessary. We use the symbol $E_{1/2}$ to refer to the half-wave potentials measured by cyclic voltammetry. The symbol E_f refers to the formal potential, which is related to the standard potential, $E°$, by the pertinent activity coefficients. For reversible or quasireversible cyclic voltammograms, $E_{1/2}$ differs insignificantly from E_f, and activity effects are occasionally neglected so that $E°$ is approximated as E_f or $E_{1/2}$. We express all potentials in acetonitrile relative to the $[Fe(Cp)_2]^{+/0}$ reference electrode in acetonitrile. This choice of reference electrodes is as recommended by the International Union of Pure and Applied Chemistry (IUPAC), and it avoids the extrathermodynamic assumptions regarding liquid junction potentials that would be introduced by the use of aqueous reference electrodes such as the normal hydrogen electrode (NHE) or the saturated calomel electrode (SCE). Such aqueous reference electrodes are widely used in presenting qualitative energy diagrams for photoelectrochemical cells,[19,20] but we choose not to introduce such uncertanties into the present paper.

Experimental Section

Reagents and Solutions. 2,2′-Bipyridyl (Aldrich), 4,4′-dimethyl-2,2′-bipyridyl (Aldrich), 5-chloro-phenanthroline (GFS Chemicals), ferrous ammonium sulfate hexahydrate (Fisher), potassium cyanide (Fisher), sodium hexafluorophosphate (Aldrich), ferric nitrate (Fisher), decamethylferrocene (Aldrich), cupric nitrate trihydrate (Fisher), iodine (J. T. Baker Chemical, Co.), silver nitrate (Fisher), nitric acid (Fisher), sulfuric acid (Fisher), acetonitrile (Fisher, certified ACS grade), acetonitrile-d_3 (Aldrich), acetone (Fisher), *n*-hexane (Fisher), methanol (Fisher), ethanol (Fisher), acetic acid (Fisher), diethyl ether (Fisher), and Sephadex LH-20-100 resin (Sigma) were used without further purification. 1,1′-Dimethylferrocene (Aldrich) was recrystallized from ethanol. Et_4NBF_4 (Aldrich) was recrystallized three times from a mixture of methanol and *n*-hexane (4:1) and dried under vacuum at 96 °C. NaI was recrystallized from ethanol/water (1:1) and dried under vacuum at 69 °C in an Abderhalden pistol for 12 h. Et_4NI (Aldrich) was recrystallized from water and dried under vacuum at 100 °C for 12 h. Solutions of NaI and Et_4NI in acetonitrile were standardized by titration with standard aqueous $AgNO_3$, with the use of Eosin as indicator.[21]

Distilled deionized water was obtained from a Barnstead NANOpure Infinity ultrapure water system. Solutions of Fe(III) complexes and iodide in acetonitrile were prepared just prior to use and kept in the dark to prevent any photochemical change. Since solutions of $[Fe^{III}(CH_3Cp)_2]PF_6$ are highly O_2 sensitive, stopped-flow kinetic studies were performed by preparing solutions of both Fe(III) and Et_4NI with argon gas purging. These solutions were then transferred via gas-tight glass syringes. For the oxidation of iodide by the other three Fe(III) complexes, the reactants are not sensitive to O_2; however, all solutions were purged with Ar or N_2 before reaction to prevent potential complications caused by O_2.

Preparation of $[Fe^{II}(bpy)_2(CN)_2]\cdot 3H_2O$. $[Fe^{II}(bpy)_2(CN)_2]\cdot 3H_2O$ was prepared following a standard procedure.[22] For the purpose of electronic spectral and electrochemical measurements, a portion of the initial products was recrystallized from concentrated sulfuric acid (96.4%). Yield of recrystallized $[Fe^{II}(bpy)_2(CN)_2]\cdot 3H_2O$: 70.4%. Anal. Calcd for $C_{22}FeH_{22}N_6O_3$: C, 55.71; H, 4.68; N, 17.72. Found: C, 55.66; H, 4.41; N, 17.67. ^{1}H NMR (400 MHz/CD_3CN): δ 8.94 (d, 2H), 8.34 (d, 2H), 8.19 (d, 2H), 7.96 (dd, 2H), 7.70 (dd, 2H), 7.31 (dd, 2H), 7.15 (dd, 2H), 6.50 (d, 2H).

Preparation of $[Fe^{III}(bpy)_2(CN)_2]NO_3\cdot 2H_2O$. Schilt's method[22] was used to prepare and recrystallize $[Fe^{III}(bpy)_2(CN)_2]NO_3\cdot 2H_2O$. Anal. Calcd for $C_{22}FeH_{20}N_7O_5$: C, 50.98; H, 3.89; N, 18.92. Found: C, 51.02; H, 3.58; N, 19.11.

Preparation of $[Fe^{II}$(4,4′-dimethyl-bipyridine)$_2(CN)_2]\cdot 3H_2O$. $[Fe^{II}$(4,4′-dimethyl-bipyridine)$_2(CN)_2]\cdot 3H_2O$ ($[Fe^{II}(dmbpy)_2(CN)_2]\cdot 3H_2O$) was prepared as described in the literature.[17] Pure $[Fe^{II}(dmbpy)_2(CN)_2]\cdot 3H_2O$ was obtained by passing a saturated ethanol solution through a column of Sephadex LH-20-100 resin, eluting with ethanol, and removing ethanol by rotary evaporation. Anal. Calcd for $C_{26}FeH_{30}N_6O_3$: C, 58.88; H, 5.70; N, 15.84. Found: C, 58.86; H, 5.58; N, 15.47. ^{1}H NMR (400 MHz/CD_3CN): δ 9.52 (d, 2H), 8.14 (s, 2H), 8.11 (s, 2H), 7.36 (d, 2H), 7.12 (d, 2H), 7.00 (d, 2H), 2.55 (s, 6H), 2.39 (s, 6H).

Preparation of $[Fe^{III}(dmbpy)_2(CN)_2]NO_3\cdot 2H_2O$. The synthesis of this Fe(III) compound was similar to that of $[Fe^{III}(bpy)_2(CN)_2]NO_3\cdot 2H_2O$. $[Fe^{II}(dmbpy)_2(CN)_2]$ was oxidized by concentrated HNO_3 to form $[Fe^{III}(dmbpy)_2(CN)_2]NO_3$. Then it was purified by recrystallization from hot distilled deionized water. Yield of $[Fe^{III}(dmbpy)_2(CN)_2]NO_3\cdot 2H_2O$: 73.1%. Anal. Calcd for $C_{26}FeH_{28}N_7O_5$: C, 54.37; H, 4.91; N, 17.07. Found: C, 54.39; H, 4.79; N, 17.24.

(9) Eberson, L. *Acta Chem. Scand.* **1984**, *B38*, 439−459.
(10) Eberson, L. *Electron Transfer Reactions in Organic Chemistry;* Springer-Verlag: New York, 1987; pp 47, 62.
(11) Grätzel, M. *Nature* **2001**, *414*, 338−344.
(12) Grätzel, M. *J. Photochem. Photobiol., A* **2004**, *164*, 3−14.
(13) Grätzel, M. *Inorg. Chem.* **2005**, *44*, 6841−6851.
(14) Nazeeruddin, M. K.; Kay, A.; Rodicio, I.; Humphry-Baker, R.; Müller, E.; Liska, P.; Vlachopoulos, N.; Grätzel, M. *J. Am. Chem. Soc.* **1993**, *115*, 6382−6390.
(15) Hansen, G.; Gervang, B.; Lund, T. *Inorg. Chem.* **2003**, *42*, 5545−5550.
(16) Ferrere, S. *Chem. Mater.* **2000**, *12*, 1083−1089.
(17) Ferrere, S. *Inorg. Chim. Acta* **2002**, *329*, 79−92.
(18) Ferrere, S.; Gregg, B. A. *J. Am. Chem. Soc.* **1998**, *120*, 843−844.
(19) Grätzel, M. *J. Photochem. Photobiol., C* **2003**, *4*, 145−153.
(20) Hagfeldt, A.; Grätzel, M. *Chem. Rev.* **1995**, *95*, 49−68.
(21) Kolthoff, I. M.; Sandell, E. B.; Meehan, E. J.; Bruckenstein, S. *Quantitative Chemical Analysis;* Macmillan: New York, 1969; pp 849−852.
(22) Schilt, A. A. *J. Am. Chem. Soc.* **1960**, *82*, 3000−3005.

Preparation of $[Fe^{III}(CH_3Cp)_2]PF_6$. $[Fe^{III}(CH_3Cp)_2]PF_6$ was prepared by following the procedure of Carney et al.[23] An amount of 0.604 g (2.73 mmol) of 1,1′-dimethylferrocene was dissolved in 5.0 mL of ether, and 2.27 g (5.62 mmol) of ferric nitrate was added to 5.0 mL of 0.04 N HCl. The two solutions were mixed together with blue color immediately appearing. Then 0.724 g (4.31 mmol) of sodium hexafluorophosphate was added to the above blue solution. The precipitate was collected by vacuum filtration, rinsed with cold dilute acid, water, and diethyl ether, and dried in a vacuum desiccator. Yield of $[Fe^{III}(CH_3Cp)_2]PF_6$: 61.1%. For UV−vis spectra and kinetic study, $[Fe^{III}(CH_3Cp)_2]PF_6$ was recrystallized from hot water and dried under vacuum for 12 h. Anal. Calcd for $C_{12}FeH_{14}PF_6$: C, 40.14; H, 3.93; F, 31.75. Found: C, 39.89; H, 3.80; F, 31.47.

Preparation of $[Fe^{II}(5\text{-Cl-phen})_2(CN)_2]\cdot 2H_2O$. $[Fe^{II}(5\text{-Cl-phen})_2(CN)_2]\cdot 2H_2O$ was prepared according to Schilt and Leman's method.[24] ^1H NMR (400 MHz/CD_3OD): δ 10.04 (dd, 1H), 9.55 (dd, 1H), 8.94 (dd, 1H), 8.70 (dd, 1H), 8.66 (d, 1H), 8.43 (dd, 2H), 8.36 (s, 1H), 8.14 (dd, 1H), 8.04 (dd, 1H), 7.66 (dd, 1H), 7.62 (dd, 1H), 7.57 (dd, 1H), 7.51 (dd, 1H).

Preparation of $[Fe^{III}(5\text{-Cl-phen})_2(CN)_2]NO_3\cdot 2H_2O$. $[Fe^{III}(5\text{-Cl-phen})_2(CN)_2]NO_3\cdot 2H_2O$ was prepared by oxidizing the crude $[Fe^{II}(5\text{-Cl-phen})_2(CN)_2]\cdot 2H_2O$ with 70% nitric acid. The Fe(III) complex was precipitated out with the addition of some amount of water. It was collected by vacuum filtration, rinsed with water to remove acid, and dried in vacuum. Yield of $[Fe^{III}(5\text{-Cl-phen})_2(CN)_2]NO_3\cdot 2H_2O$: 51.0%. Anal. Calcd for $C_{26}FeH_{18}N_7Cl_2O_5$: C, 49.16; H, 2.86; N, 15.43. Found: C, 49.37; H, 2.66; N, 15.47. This compound is relatively unstable, decomposing significantly over several months even when kept under vacuum in the dark.

Methods. All single UV−vis spectra were recorded on a HP-8453 diode-array spectrophotometer with 1.0 cm rectangular quartz cells, equipped with Brinkman Lauda RM6 thermostated water bath to maintain the temperature at 25.0 ± 0.1 °C. Cyclic voltammograms (CV) and Osteryoung square wave voltammograms (OSWV) were recorded at room temperature on a BAS 100 B electrochemical analyzer with scan rate of 100 mV/s, equipped with BAS cell stand C3 with purging and stirring system, using a glassy-carbon working electrode, Ag/AgCl (saturated aqueous KCl) reference electrode, and a Pt wire auxiliary electrode. In acetonitrile, the half-wave potential of $[Fe(Cp)_2]^{+/0}$ is close to that of $[Fe(dmbpy)_2(CN)_2]^{+/0}$, so decamethylferrocene was used as the internal reference in all CV and OSWV experiments. The half-wave potentials of the four Fe(III/II) complexes are expressed versus $[Fe(Cp)_2]^{+/0}$ in this paper by applying a correction of 504 mV (vide infra). ^1H NMR spectra were recorded on a Bruker AV 400 spectrometer. For fast reactions, kinetic studies were performed by mixing equal volumes of the two reactants on a Hi-Tech Scientific model SF-51 stopped-flow apparatus in the 1.0 cm optical path configuration. The instrument was equipped with an SU-40 spectrophotometer unit and a C-400 circulatory water bath. An OLIS 4300S system was used for data acquisition and analysis. Reactions were monitored at a fixed wavelength, and the rate constants were obtained by fitting the data with OLIS-supplied first-order functions. For slow reactions, equal volumes of the two reactants were mixed in a 1 cm rectangular cuvette, and then kinetic studies were immediately performed on an HP-8453 diode-array spectrophotometer equipped with a RM6 Lauda circulatory water bath; appropriate UV cutoff filters were placed in the optical beam to minimize photolysis. Rate constants (k_{obs}) were obtained by fitting the experimental data with the software that was provided by HP. The temperature was maintained at 25.0 ± 0.1 °C. The Prism 4 computer software package was used to fit the overall rate law to the values of k_{obs} with $1/Y^2$ weighting.

Table 1. UV−Visible Absorbance and Electrochemical Characteristics of the Iron Complexes in CH_3CN

compounds	band	λ_{max} nm	ϵ $M^{-1}\,cm^{-1}$	$E_{1/2}$ mV[a]	$\Delta E_{p/p}$ mV
$[Fe^{II}(bpy)_2(CN)_2]$	I	388	6.99×10^3	+70 ± 2	72
	II	605	7.36×10^3		
$[Fe^{III}(bpy)_2(CN)_2]NO_3$	I	301	2.50×10^4		
	II	503	226		
$[Fe^{II}(dmbpy)_2(CN)_2]$	I	383	7.37×10^3	−36 ± 2	62
	II	608	6.93×10^3		
$[Fe^{III}(dmbpy)_2(CN)_2]NO_3$	I	356	3.88×10^3		
$[Fe^{II}(CH_3Cp)_2]$	I	324	76	−108 ± 2	82
	II	438	110		
$[Fe^{III}(CH_3Cp)_2]PF_6$	I	650	354		
$[Fe^{II}(5\text{-Cl-phen})_2(CN)_2]$	I	375	2.1×10^3	168 ± 2	91
	II	609	1.07×10^4		
$[Fe^{III}(5\text{-Cl-phen})_2(CN)_2]NO_3$	I	362	3.74×10^3		

[a] $E_{1/2}$ vs $[Fe(Cp)_2]^{+/0}$, at room temperature (~22 °C) and μ = 0.10 M (Et_4NBF_4).

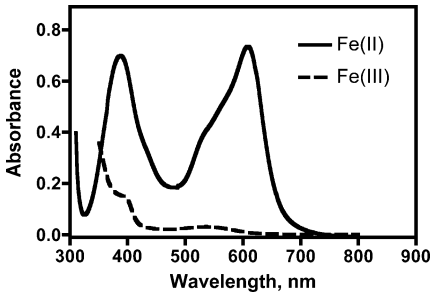

Figure 1. UV−visible spectra of 0.10 mM $[Fe^{II}(bpy)_2(CN)_2]$ and 0.10 mM $[Fe^{III}(bpy)_2(CN)_2]NO_3$ in acetonitrile.

Results

1. UV−Visible Spectra. The UV−visible absorbance characteristics of all the iron complexes in CH_3CN are shown in Table 1. The reported spectral properties were obtained from solutions of the pure compounds except for $[Fe^{II}(5\text{-Cl-phen})_2(CN)_2]$. A solution of the latter compound was prepared by quantitative reduction of $[Fe^{III}(5\text{-Cl-phen})_2(CN)_2]^+$ with $[Fe^{II}(CH_3Cp)_2]$; the $[Fe^{III}(CH_3Cp)_2]^+$ product has negligible absorbance at the wavelengths reported for $[Fe^{II}(5\text{-Cl-phen})_2(CN)_2]$. The spectra of $[Fe^{II}(bpy)_2(CN)_2]$, $[Fe^{II}(dmbpy)_2(CN)_2]$, $[Fe^{II}(CH_3Cp)_2]$, $[Fe^{III}(CH_3Cp)_2]^+$, and $[Fe^{II}(5\text{-Cl-phen})_2(CN)_2]$ are very close to the spectra of previous reports.[17,25−27] Figure 1 shows the UV−visible spectra of 0.10 mM $[Fe^{II}(bpy)_2(CN)_2]$ and 0.10 mM $[Fe^{III}(bpy)_2(CN)_2]NO_3$ in acetonitrile. For $[Fe^{II}(bpy)_2(CN)_2]$, there are two characteristic absorbance peaks at 388 and 605 nm, for which the extinction coefficients (ϵ) are 6988 and 7360 $M^{-1}\,cm^{-1}$; for $[Fe^{III}(bpy)_2(CN)_2]NO_3$, the absorbance at 605 nm is nearly zero. Iodide does not absorb in the visible range, and triiodide (I_3^-), one of products of the reaction (see

(23) Carney, M. J.; Lesniak, J. S.; Likar, M. D.; Pladziewicz, J. R. *J. Am. Chem. Soc.* **1984**, *106*, 2565−2569.
(24) Schilt, A. A.; Leman, T. W. *J. Am. Chem. Soc.* **1967**, *89*, 2012−2014.
(25) Barr, T. H.; Watts, W. E. *J. Organomet. Chem.* **1968**, *15*, 177−185.
(26) Burgess, J. *Spectrochim. Acta* **1970**, *26A*, 1369−1374.
(27) Pladziewicz, J. R.; Brenner, M. S.; Rodeberg, D. A.; Likar, M. D. *Inorg. Chem.* **1985**, *24*, 1450−1453.

Chart 1. Structures of the Three Potential Isomers of *cis*-[Fe^{II}(5-Cl-phen)$_2$(CN)$_2$][a]

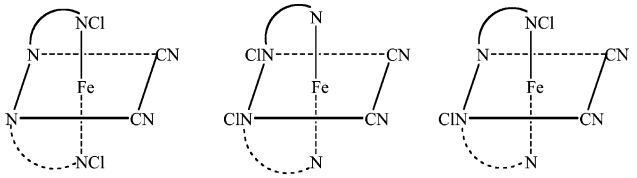

[a] ClN represents the Cl-substituted side of the 5-Cl-phen ligand.

below), has a characteristic absorbance at 363 nm (ϵ_{363} = 26 250 M^{-1} cm^{-1}; $\epsilon_{605} \approx 10$ M^{-1} cm^{-1}). Thus, for the stopped-flow experiments on the oxidation of iodide by [Fe^{III}(bpy)$_2$(CN)$_2$]NO_3, the growth of [Fe^{II}(bpy)$_2$(CN)$_2$] was monitored at 605 nm. The spectral features for the oxidation of iodide by [Fe^{III}(dmbpy)$_2$(CN)$_2$]NO_3 and [Fe^{III}(5-Cl-phen)$_2$(CN)$_2$]NO_3 are quite similar to those for the reaction of [Fe^{III}(bpy)$_2$(CN)$_2$]$^+$, and hence these reactions were monitored at 608 and 609 nm, respectively. With [Fe^{III}(CH_3Cp)$_2$]PF_6 as the oxidant, the loss of oxidant at 650 nm was monitored because of the low absorbance of [Fe^{II}(CH_3Cp)$_2$].

2. Electrochemistry. All of the electrochemical measurements were performed in acetonitrile with 0.10 M Et_4NBF_4 as the background electrolyte and 1.0 mM decamethylferrocene as an internal reference. In general, the CVs were quasireversible and had $E_{1/2}$ values within 2 mV of the OSWV peak potentials. The OSWV of a mixture of 0.50 mM ferrocene and 0.40 mM decamethylferrocene shows that $E_{1/2}$ of [Fe(Cp)$_2$]$^{+/0}$ is 504 mV (vs [Fe(Cp*)$_2$]$^{+/0}$), the same as in prior reports.[28,29] Accordingly, a correction of 504 mV is applied to the measured potentials to obtain data relative to [Fe(Cp)$_2$]$^{+/0}$. In the cases of [Fe^{II}(bpy)$_2$(CN)$_2$], [Fe^{II}(dmbpy)$_2$(CN)$_2$], and [Fe^{II}(CH_3Cp)$_2$], electrochemical data were recorded with 1.0 mM Fe(II). For [Fe^{II}(5-Cl-phen)$_2$(CN)$_2$], the Fe(II) concentration was 0.20 mM. The electrochemical results are summarized in Table 1. In the case of [Fe(CH_3Cp)$_2$], the $E_{1/2}$ is in good agreement with the literature,[28] but in the case of [Fe^{II}(dmbpy)$_2$(CN)$_2$], there is a 58 mV disagreement.[17] We attribute the disagreement for [Fe^{II}(dmbpy)$_2$(CN)$_2$] to low purity of the literature sample, as evidenced by the poor reported elemental analysis.[17] Overall, the half-wave potentials shown in Table 1 indicate that the four iron(III) complexes constitute a series of singly charged one-electron oxidants with $E_{1/2}$ values smoothly spanning a 276 mV range.

3. ^{1}H NMR Spectra. The ^{1}H NMR spectra of [Fe^{II}(bpy)$_2$(CN)$_2$], [Fe^{II}(dmbpy)$_2$(CN)$_2$], and [Fe(CH_3Cp)$_2$] in CD_3CN are readily assigned in view of the cis geometries of these species, and they give no evidence for impurities. In the case of *cis*-[Fe^{II}(5-Cl-phen)$_2$(CN)$_2$], there are potentially three isomers, as shown in Chart 1. The ^{1}H NMR spectrum (Figure S-1, Supporting Information) of 1.0 mM [Fe^{II}(5-Cl-phen)$_2$(CN)$_2$] in CD_3OD has 14 peaks with the same intensity, indicating that the compound is isomer **C**.

4. Metal-Ion Catalysis and Inhibition. We previously reported that the oxidation of iodide by [Fe^{III}(bpy)$_2$(CN)$_2$]$^+$ in acetonitrile is catalyzed by trace levels of Cu^{2+}.[1] In brief, when no precautions are taken to prevent Cu^{2+} catalysis, the reaction rates are mildly irreproducible and non-pseudo-first-order. The addition of 1.0 μM $Cu(NO_3)_2$ leads to a 54-fold decrease in the half-life, while 5.0 μM $Ni(NO_3)_2$ and $Fe(NO_3)_3$ have no effect. We now report, as summarized in Table S-1, that oxidation of iodide by the other three Fe^{III} complexes described in this study is also copper-catalyzed. For a typical reaction of 2.0 mM iodide with 50.0 μM [Fe^{III}(dmbpy)$_2$(CN)$_2$]NO_3 in 0.10 M Et_4NBF_4 at 25.0 °C, the half-life for the formation of [Fe^{II}(dmbpy)$_2$(CN)$_2$] decreased by a factor of 33 upon the addition of 1.0 μM $Cu(NO_3)_2$. For the oxidation of 80.0 mM I^- by 0.25 mM [Fe^{III}(CH_3Cp)$_2$]PF_6 in 0.02 M Et_4NBF_4 at 25.0 °C, the half-life for the formation of [Fe^{II}(CH_3Cp)$_2$] decreased 8-fold when 5.0 μM $Cu(NO_3)_2$ was deliberately added. For the oxidation of 0.20 mM I^- by 10.0 μM [Fe^{III}(5-Cl-phen)$_2$(CN)$_2$]NO_3 in 0.10 M Et_4NBF_4 at 25.0 °C, the half-life for the formation of [Fe^{II}(5-Cl-phen)$_2$(CN)$_2$] decreased by a factor of 4 because of the addition of 1.0 μM $Cu(NO_3)_2$. The degree of catalysis is not strictly comparable in these experiments, because different iodide concentrations were used for the different oxidants. Nevertheless, these results show that copper catalysis of iodide oxidation in acetonitrile is a rather general phenomenon and not dependent on the presence of cyanide in the coordination sphere of the oxidant.

Our prior communication also mentioned that bpy and ethylenediamine are effective inhibitors of copper catalysis in the oxidation of iodide by [Fe(bpy)$_2$(CN)$_2$]$^+$ in acetonitrile.[1] The specific results are as follows: when 1.0 or 5.0 mM bpy was added to the reactants (2.0 mM NaI, 50.0 μM [Fe^{III}(bpy)$_2$(CN)$_2$]NO_3, 0.098 mM Et_4NBF_4), the half-life was 4.6 s, that is, ~6-fold greater than in the absence of bpy. Ethylenediamine (en) was also tested as an inhibitor of copper catalysis. When 1.0 mM en was added to the same concentration of the above reactants, the half-life was 4.52 s, that is, effectively the same as with bpy. However, the direct oxidation of en by [Fe^{III}(bpy)$_2$(CN)$_2$]NO_3 occurs with a 700 s half-life (0.05 mM [Fe^{III}(bpy)$_2$(CN)$_2$]NO_3 and 1.0 mM en in acetonitrile), while no reaction takes place between [Fe^{III}(bpy)$_2$(CN)$_2$]NO_3 and bpy. Thus bpy, rather than en, was used in all subsequent experiments as an inhibitor of copper catalysis. The addition of bpy as an inhibitor also leads to excellent pseudo-first-order kinetic traces for all four of the Fe(III) oxidants, as we have already shown in the case of [Fe^{III}(bpy)$_2$(CN)$_2$]NO_3.[1]

5. Kinetic Effects of Water. Experiments directed toward assessing the kinetic effects of small amounts of water are described in Supporting Information. In brief, they show that such effects are normally negligible under the nominally anhydrous conditions employed in this study. Therefore, for all subsequent kinetic studies, acetonitrile was used directly, without any further drying. On the other hand, NaI is relatively hygroscopic and was found to introduce enough

(28) Nelsen, S. F.; Wang, Y.; Ramm, M. T.; Accola, M. A.; Pladziewicz, J. R. *J. Phys. Chem.* **1992**, *96*, 10654−10658.
(29) Noviandri, I.; Brown, K. N.; Fleming, D. S.; Gulyas, P. T.; Lay, P. A.; Masters, A. F.; Phillips, L. *J. Phys. Chem. B* **1999**, *103*, 6713−6722.

water to perturb the kinetics when used as an iodide source; consequently, nonhygroscopic Et_4NI was used in all kinetic studies reported below.

6. Product Identification and Stoichiometry. Products of the bpy-inhibited reactions of I^- with the Fe(III) complexes were identified qualitatively, and quantitative determinations of the stoichiometry were also performed. In general, the metal complexes undergo simple one-electron reduction, while the iodide is oxidized to triiodide as in

$$2Fe(III) + 3I^- \rightarrow 2Fe(II) + I_3^- \qquad (1)$$

In the case of $[Fe^{III}(bpy)_2(CN)_2]NO_3$, the products were identified and quantitated by UV−vis spectrophotometry. The UV−vis spectrum (Figure S-4) of the product solution of 2.0 mM NaI and 50.0 μM $[Fe^{III}(bpy)_2(CN)_2]NO_3$ in CH_3CN, with 0.10 M Et_4NBF_4 and 5.0 mM bpy at 25 °C, shows that there are two peaks at 369 and 605 nm. The peak at 605 nm is readily assigned to $[Fe^{II}(bpy)_2(CN)_2]$ (see Table 1). We find that I_3^- has a characteristic absorbance at 363 nm with an extinction coefficient of 2.62×10^4 M^{-1} cm^{-1} (differing by only 4% from Isci and Mason's result[31]), while $[Fe^{II}(bpy)_2(CN)_2]$ also absorbs in the same region. Quantitative dual-wavelength analysis at 605 and 369 nm ($\epsilon_{605} = 7360$ and $\epsilon_{369} = 5713$ M^{-1} cm^{-1} for $[Fe^{II}(bpy)_2(CN)_2]$, $\epsilon_{605} \approx 0$ and $\epsilon_{369} = 25\,180$ M^{-1} cm^{-1} for I_3^-) demonstrated that the yield of $[Fe^{II}(bpy)_2(CN)_2]$ is 99% and that the product ratio of $[I_3^-]/[Fe(II)]$ is 0.48 ± 0.03. These results are in excellent agreement with reaction 1.

Quite similar results were obtained with $[Fe^{III}(dmbpy)_2(CN)_2]NO_3$ as the oxidant. The product solution of 5.0 mM Et_4NI and 47.0 μM $[Fe^{III}(dmbpy)_2(CN)_2]NO_3$ in CH_3CN, with 5.0 mM bpy, at ionic strength (μ) of 0.10 M and at 25 °C, has a UV−vis spectrum (Figure S-5) with two peaks at 368 and 605 nm, indicative that the products of the reaction are I_3^- and $[Fe^{II}(dmbpy)_2(CN)_2]$; the 3 nm spectral shift for Fe(II) (compared to Table 1) is likely due to differing amounts of water in the samples.[30] Dual wavelength analysis (368 and 605 nm) provides a ratio of 0.43 ± 0.03 for $[I_3^-]/[Fe(II)]$, also consistent with reaction 1.

With $[Fe^{III}(CH_3Cp)_2]PF_6$ as the oxidant, both UV−vis and ^1H NMR spectra were used. The ^1H NMR spectrum of the product solution (80.0 mM NaI, 2.5 mM $[Fe^{III}(CH_3Cp)_2]PF_6$, 10.0 mM bpy, and 20.0 mM Et_4NBF_4), shown in Figure 2, demonstrates that $[Fe^{II}(CH_3Cp)_2]$ is one of the products (singlets at δ 3.94 and 1.95 ppm, in agreement with the authentic material);[32] comparison of the peak integrals for Et_4N^+ and $[Fe(CH_3Cp)_2]$ gives the yield of $[Fe(CH_3Cp)_2]$ as 99 ± 1%. The UV−vis spectrum of the product solution (Figure 3) (5.0×10^{-3} M NaI, 1.0×10^{-4} M $[Fe^{III}(CH_3Cp)_2]PF_6$, 10.0 mM bpy, at $\mu = 0.10$ M (Et_4NBF_4) and 25 °C) has a strong absorbance at 363 nm arising from I_3^- ($\epsilon_{363} \approx 8$ M^{-1} cm^{-1} for $[Fe^{II}(CH_3Cp)_2]$). The yield of I_3^- was determined from the UV−vis spectrum, which led to a calculated product ratio of $\Delta[I_3^-]/\Delta[Fe^{II}(CH_3Cp)_2]$ equal to 0.45. Therefore, eq 1 accurately describes this reaction.

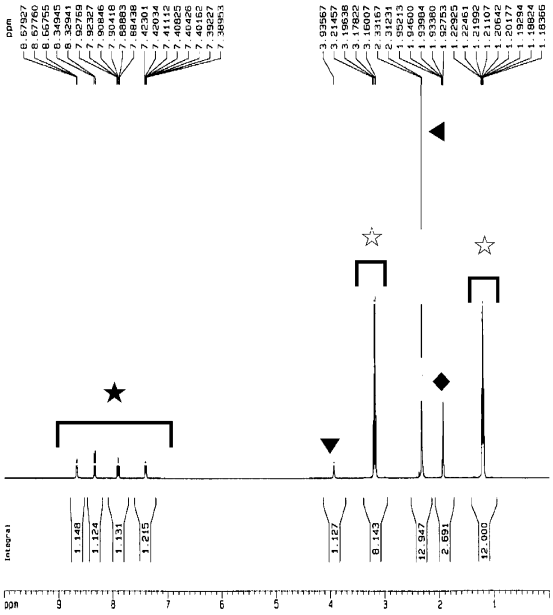

Figure 2. ^1H NMR spectrum of product solution of the oxidation of 80.0 mM NaI by 2.5 mM $[Fe^{III}(CH_3Cp)_2]PF_6$ in CD_3CN, in the presence of 10.0 mM bpy and 20.0 mM Et_4NBF_4: ★, bpy; ☆, Et_4NBF_4; ▼, $[Fe(CH_3Cp)_2]$; left solid triangle, H_2O; ◆, overlap of CD_3CN and $-CH_3$ in $[Fe(CH_3Cp)_2]$.

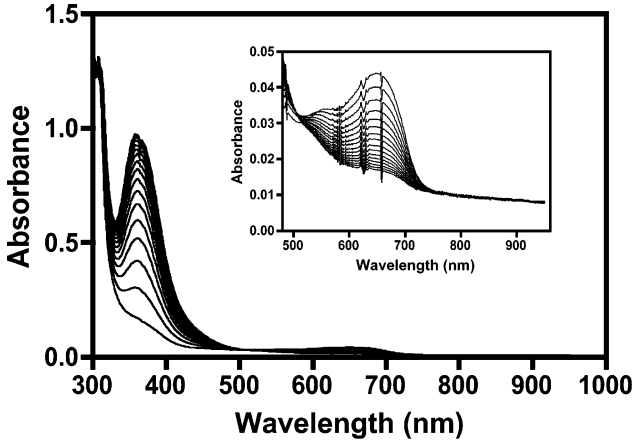

Figure 3. UV−vis spectra for the oxidation of 5.0 mM NaI by 0.10 mM $[Fe^{III}(CH_3Cp)_2]PF_6$ in CH_3CN, in the presence of 10.0 mM bpy, at $\mu = 0.10$ M (Et_4NBF_4) and 25 °C, 60 s interval between spectra. (Inset shows the enlarged spectra from 480 to 950 nm.)

The reaction of $[Fe^{III}(5\text{-Cl-phen})_2(CN)_2]NO_3$ was examined by ^1H NMR and UV−vis spectra. The aromatic region of the product ^1H NMR spectrum (Figure S-6) (0.50 mM $[Fe^{III}(5\text{-Cl-phen})_2(CN)_2]NO_3$, 3.0 mM Et_4NI, 2.0 mM bpy) is dominated by four peaks of equal intensity arising from the free bpy. The same region also displays a set of 14 small peaks with the same intensity, characteristic of isomer **C** of $[Fe^{II}(5\text{-Cl-phen})_2(CN)_2]$. The UV−vis spectrum of the product solution shown in Figure S-7 confirms the formation of I_3^- and $[Fe^{II}(5\text{-Cl-phen})_2(CN)_2]$. Determination of the yield of I_3^- and Fe(II) by spectrophotometric analysis at 363 and 609 nm ($[Fe(III)] = 50.0$ μM, $[Et_4NI] = 10.0$ mM, $[bpy] = 5.0$ mM, and $[Et_4NBF_4] = 0.09$ M) indicates that the stoichiometric ratio of $\Delta[I_3^-]/\Delta[Fe^{II}(5\text{-Cl-phen})_2(CN)_2^+]$ is

(30) Toma, H. E.; Takasugi, M. S. *J. Solution Chem.* **1983**, *12*, 547−561.
(31) Isci, H.; Mason, W. R. *Inorg. Chem.* **1985**, *24*, 271−274.
(32) Materikova, R. B.; Babin, V. N.; Lyatifov, I. R.; Kurbanov, T. K.; Fedin, E. I.; Petrovskii, P. V.; Lutsenko, A. I. *J. Organomet. Chem.* **1977**, *142*, 81−87.

0.46 ± 0.02. Thus, the stoichiometric ratio of the reaction complies with eq 1, too.

7. Reaction of Iodine with 2,2′-Bipyridine. From spectroscopic and conductivity studies it is well-known that iodine reacts with π-donors such as pyridine to form I_3^-.[33] Similar interactions have been inferred to explain the strong effects of bpy on the voltammetry of I^- in acetonitrile.[3] It is now believed that I_3^- is produced in a very fast (nanosecond) equilibrium as in

$$2\text{bpy} + 2I_2 \rightleftharpoons \text{bpy}_2I^+ + I_3^- \quad (2)$$

Additional I_3^- is then produced in a slow as-yet undefined reaction.[33] This raises the possibility that bpy/iodine interactions are important in the present reaction system. First, UV−vis spectra of 0.60 mM I_2 in air-saturated acetonitrile were recorded, which showed that the solution is stable for more than 60 min. Then a solution containing 0.20 mM I_2 and 5.0 mM bpy was prepared anaerobically, and UV−vis spectra were recorded. These spectra showed the slow formation of 0.027 mM I_3^- with a half-life of about 580 s. We infer that the equilibrium constant for reaction 2 is unfavorable under the dilute conditions of the above experiment. The large equilibrium constant for association of I^- with I_2 to produce triiodide in acetonitrile (reaction 3, pK = −7.18)[4] further ensures that reaction 2 will be shifted to the left, such that it is insignificant in the Fe(III)/I^- reactions reported herein.

$$I_2 + I^- \rightleftharpoons I_3^- \quad (3)$$

The fact that the Fe(III)/I^- reaction kinetics are independent of the bpy concentration (vide supra) further supports the conclusion that I_2/bpy interactions are insignificant in the current study.

8. Kinetics of I^- Oxidation by Fe(III). Kinetics studies were generally performed with a large (pseudo-first-order) excess of Et_4NI over Fe(III), under anaerobic conditions with the temperature being held at 25.0 °C, the ionic strength at 0.10 M (Et_4NBF_4), and with a significant concentration of free bpy to suppress copper catalysis. Rates were determined spectrophotometrically as the loss of Fe(III) or gain of Fe(II). The kinetic traces generally yielded excellent pseudo-first-order fits, and the derived pseudo-first-order rate constants, k_{obs}, were reproducible to ±5%.

With $[Fe^{III}(bpy)_2(CN)_2]NO_3$ as the oxidant, the values of k_{obs} (Table S-3) increase with increasing iodide concentration, but the dependence is nonlinear. As shown in Figure 4, a linear relationship is obtained when $k_{obs}/[I^-]$ is plotted as a function of $[I^-]$. The corresponding rate law is

$$k_{obs} = 2(k_1[I^-] + k_2[I^-]^2) \quad (4)$$

and the slope and intercept of the plot of $k_{obs}/[I^-]$ vs $[I^-]$ yield values for k_1 and k_2 of $(2.9 \pm 0.1) \times 10^1$ M^{-1} s^{-1} and $(3.88 \pm 0.14) \times 10^3$ M^{-2} s^{-1}, respectively.

Qualitatively, the reaction of $[Fe^{III}(dmbpy)_2(CN)_2]NO_3$ is substantially slower than that of $[Fe^{III}(bpy)_2(CN)_2]NO_3$, although the rate law has the same form. Values of k_{obs} are given in Table S-4, and the derived values of k_1 and k_2 are given in Table 2.

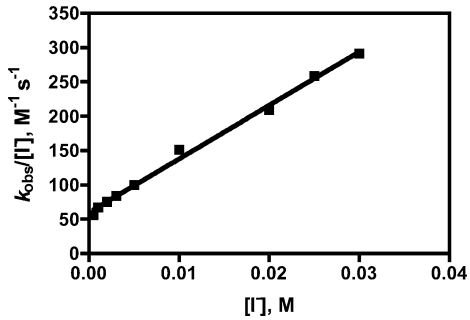

Figure 4. Plot of $k_{obs}/[I^-]$ vs $[I^-]$ for the reaction between 0.05 mM $[Fe^{III}(bpy)_2(CN)_2]NO_3$ and various concentrations of Et_4NI at μ = 0.10 M and 25 °C, in the presence of 5.0 mM 2,2′-bipyridine.

The fastest reaction is that of $[Fe^{III}(5\text{-Cl-phen})_2(CN)_2]NO_3$, which is also the most powerful oxidant in the series. Because of the large rate constants, iodide concentrations were kept low, and thus the derived value of k_2 is relatively imprecise. Values of k_{obs} are given in Table S-5, and the derived values of k_1 and k_2 are given in Table 2.

With $[Fe^{III}(CH_3Cp)_2]PF_6$ as the oxidant, extra care had to be taken to exclude air, since this oxidant is rather sensitive to O_2; the half-life for the decomposition of 1.0 mM $[Fe^{III}(CH_3Cp)_2]PF_6$ in air-saturated acetonitrile is comparable to that for the reduction by lower concentrations of iodide. Initial Fe(III) concentrations were 5−25 times higher than those with the other oxidants because of the low absorptivity of $[Fe^{III}(CH_3Cp)_2]^+$. This oxidant is also the weakest of the four described in this report, which leads to the lowest rates of reaction with iodide and only a minor contribution from the k_1 term in the rate law. As a consequence of these factors, the value of k_1 is relatively imprecise. Values of k_{obs} are given in Table S-6, and the derived values of k_1 and k_2 are given in Table 2.

Although the above kinetic results give no indication of significant product inhibition, a deliberate test for this effect was conducted for the reaction of $[Fe^{III}(bpy)_2(CN)_2]^+$. This test was conducted by performing the reaction with the initial concentration of $[Fe^{II}(bpy)_2(CN)_2]$ ranging from 15 to 60 μM, the other concentrations being held at 7.5 μM $[Fe^{III}(bpy)_2(CN)_2]NO_3$ and 75 μM Et_4NI. Under these conditions, the reactions still display pseudo-first-order behavior, but the values of k_{obs} decrease significantly as the concentration of $[Fe^{II}(bpy)_2(CN)_2]$ increases (Table S-7). As shown in Figure 5, a plot of $1/k_{obs}$ vs $[Fe^{II}(bpy)_2(CN)_2]$ is linear, consistent with eq 5:

$$1/k_{obs} = m[\text{Fe(II)}] + b \quad (5)$$

A fit to eq 5 gives $m = (3.07 \pm 0.30) \times 10^6$ M^{-1} s and b = 200 ± 8.7 s under the specified conditions. These results show that kinetic inhibition by Fe(II) is negligible when no Fe(II) is initially present.

Discussion

Although not the focus of the present report, our results on copper catalysis show that this phenomenon is much

(33) Tassaing, T.; Besnard, M. *J. Phys. Chem. A* **1997**, *101*, 2803−2808.

Table 2. Rate Constants for the Oxidation of Iodide by Fe(III) Complexes in Acetonitrile[a]

oxidants	E_f, mV[b]	k_1, M^{-1} s^{-1}	k_2, M^{-2} s^{-1}
$[Fe(CH_3Cp)_2]PF_6$	-108 ± 2	0.05 ± 0.01	27.1 ± 1.0
$[Fe(dmbpy)_2(CN)_2]NO_3$	-36 ± 2	0.65 ± 0.05	$(3.46 \pm 0.16) \times 10^2$
$[Fe(bpy)_2(CN)_2]NO_3$	$+70 \pm 2$	29.2 ± 0.82	$(3.88 \pm 0.14) \times 10^3$
$[Fe(5\text{-}Cl\text{-}phen)_2(CN)_2]NO_3$	168 ± 2	$(1.45 \pm 0.03) \times 10^3$	$(1.68 \pm 0.11) \times 10^5$

[a] With 5.0 mM bpy and $\mu = 0.10$ M (Et_4NBF_4), at 25 °C. [b] E_f vs $[Fe(Cp)_2]^{+/0}$, approximated as $E_{1/2}$.

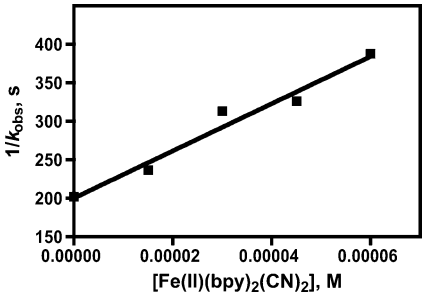

Figure 5. Plot of $1/k_{obs}$ vs $[Fe^{II}(bpy)_2(CN)_2]$ for the reaction between 7.5 μM $[Fe^{III}(bpy)_2(CN)_2]NO_3$ and 75 μM Et_4NI in acetonitrile, with 0.10 M Et_4NBF_4 and 5.0 mM bpy, at 25.0 °C.

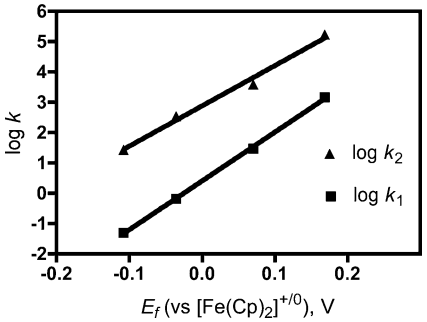

Figure 6. Plots of log k vs E_f for the oxidation of I^- by $[Fe^{III}(5\text{-}Cl\text{-}phen)_2(CN)_2]^+$, $[Fe^{III}(bpy)_2(CN)_2]^+$, $[Fe^{III}(dmbpy)_2(CN)_2]^+$, and $[Fe^{III}(CH_3Cp)_2]^+$ in CH_3CN.

broader than we initially reported.[1] It is significant in all four of the reactions where iodide is oxidized by substitution-inert Fe(III) reagents in acetonitrile. When the oxidants are of the $Fe^{III}L_2(CN)_2$ type, there is the possibility that catalysis occurs through the formation of oligonuclear cyanide-bridged Fe−Cu complexes.[34] That the reaction of $[Fe(CH_3Cp)_2]^+$ is also copper-catalyzed, however, suggests the operation of a more general mechanism of catalysis. A ping-pong mechanism involving Cu(I) and Cu(II) is a possibility, but further speculation awaits a detailed kinetic study.

Estimates of the equilibrium constants for the overall reactions (eq 1) can be obtained from the differences between the standard potentials of the Fe(III)/Fe(II) and I_3^-/I^- redox couples. $E°$ values for the Fe(III)/Fe(II) half cells can be approximated as the $E_{1/2}$ values given in Table 1. The $E°$ value for the I_3^-/I^- couple has been the subject of several reports. In a voltammetric study, Popov and Geske obtained $E°(I_3^-/I^-) = -0.27$ V vs $Ag/AgNO_3$(0.01 M, AN);[3] correcting this to the $Fe(Cp)^{+/0}$ reference electrode by −0.089 V[35] leads to $E°(I_3^-/I^-) = -0.36$ V. Desbarres used potentiometry to obtain $E_f(I_3^-/I^-) = -0.248$ V vs $Ag/AgNO_3$(0.01 M, AN) or −0.337 V vs $Fe(Cp)_2^{+/0}$ at $\mu = 0.1$ M,[36] which is similar to the result of Popov and Geske. Nelson and Iwamoto used voltammetry to obtain $E_f(I_3^-/I^-) = 0.06$ V vs SCE at $\mu = 0.1$ M;[37] a correction of 0.30 V for $E°(Ag/AgNO_3$, 0.01 M, AN) vs $E°$(SCE)[38] plus the above correction for $E°(Ag/AgNO_3)$ to $E°(Fe(Cp)_2^{+/0})$ leads to $E_f(I_3^-/I^-) = -0.329$ V vs $Fe(Cp)_2^{+/0}$ at $\mu = 0.1$ M, which is in moderate agreement with the above two reports. Most recently, Benoit reported $E°(I_3^-/I^-) = -0.315$ V vs $Fe(Cp)_2^{+/0}$.[39] Thus there is a 45 mV range in the reported $E°$ values; we use the average value, $E°(I_3^-/I^-) = -0.34 \pm 0.02$ V vs $Fe(Cp)_2^{+/0}$. Clearly, the equilibrium constants for reaction 1 are highly favorable for all four Fe(III) oxidants. Interestingly, the equilibrium constant for reduction of I_2 by $[Fe(CH_3Cp)_2]$ is also favorable, but this seeming paradox is explained by the large association constant to form I_3^-, such that I_2 is reduced only as far as I_3^-.[40]

Given the similarity of the stoichiometry and rate law for these reactions in acetonitrile to those for typical aqueous outer-sphere iodide oxidations, an analogous mechanism is proposed:

$$Fe(III) + I^- \rightleftharpoons Fe(II) + I^\bullet \qquad k_1, k_{-1}, K_1 \qquad (6)$$

$$Fe(III) + 2I^- \rightleftharpoons Fe(II) + I_2^{-\bullet} \qquad k_2, k_{-2}, K_2 \qquad (7)$$

$$I^\bullet + I^- \rightleftharpoons I_2^{-\bullet} \qquad k_3, k_{-3}, K_{rad} \qquad (8)$$

$$I_2^{-\bullet} + Fe(III) \rightarrow I_2 + Fe(II) \qquad k_4 \qquad (9)$$

$$I^- + I_2 \rightleftharpoons I_3^- \qquad K_{eq} \qquad (10)$$

This mechanism leads to the observed overall reaction (eq 1), and if it is assumed that the k_1 and k_2 steps are irreversible and that the following reactions are rapid, it leads to the observed rate law, eq 4. The hemicolligation of $I^\bullet$ with I^- (K_{rad}) is well-known and essentially diffusion-controlled in aqueous solution; in acetonitrile this reaction is likewise known to be diffusion controlled, and its equilibrium constant is believed to be at least 100 times greater than in water.[6]

The driving force dependences of k_1 and k_2 are displayed in Figure 6 as plots of log k vs E_f(Fe(III)/Fe(II)). Both of these plots are linear (LFERs), and their slopes are 16.1 and 13.3 V^{-1}, respectively. A slope of 16.9 V^{-1} for the plot of

(34) Comte, V.; Vahrenkamp, H. *J. Organomet. Chem.* **2001**, *627*, 153−158.
(35) Gritzner, G. *Pure Appl. Chem.* **1990**, *62*, 1839−1858.
(36) Desbarres, J. *Bull. Soc. Chim. Fr.* **1961**, 502−506.
(37) Nelson, I. V.; Iwamoto, R. T. *J. Electroanal. Chem.* **1964**, *7*, 218−221.
(38) Larson, R. C.; Iwamoto, R. T.; Adams, R. N. *Anal. Chim. Acta* **1961**, *25*, 371−374.
(39) Benoit, R. L. *Inorg. Nucl. Chem. Lett.* **1968**, *4*, 723−729.
(40) Ishikawa, K.; Fukuzumi, S.; Tanaka, T. *Inorg. Chem.* **1989**, *28*, 1661−1665.

log k_1 would occur if all four reactions had the same value for k_{-1}. This circumstance would occur if the values of k_{-1} are at the diffusion limit, and the agreement between the observed and theoretical slopes suggests that this is the case. The slope of 13.3 V^{-1} for log k_2 requires that the values of k_{-2} vary in a systematic way with E_f, and hence the values of k_{-2} must be significantly below the diffusion limit.

Further insight can be obtained by a consideration of the observed kinetic inhibition by Fe(II) in the reaction of $[Fe(bpy)_2(CN)_2]^+$ (Figure 5). If it is assumed in the above mechanism that steps 6 and 7 are reversible and that the steady-state approximation can be made for the concentrations of $I^\bullet$ and $I_2^{-\bullet}$, the following rate law can be derived (see Supporting Information):

$$-\frac{d[Fe(III)]}{dt} = \{2\{k_1k_3k_4 + k_2k_4k_{-1}[Fe(II)] + k_2k_3k_4[I^-]\}[Fe(III)]^2[I^-]^2\}/\{k_{-2}k_{-1}[Fe(II)]^2 + k_4k_{-1}[Fe(II)][Fe(III)] + k_{-2}k_3[I^-][Fe(II)] + k_3k_4[Fe(III)][I^-] + k_{-1}k_{-3}[Fe(II)]\} \quad (11)$$

With the further approximations that $k_4[Fe(III)] \gg k_{-2}[Fe(II)]$ and $k_4[Fe(III)] \gg k_{-3}$, which should be suitable under the conditions of the experiments summarized in Figure 5, eq 11 simplifies to

$$\text{rate} = \left(\frac{2k_1k_3}{k_{-1}[Fe(II)] + k_3[I^-]} + 2k_2\right)[Fe(III)][I^-]^2 \quad (12)$$

With a pseudo-first-order excess of iodide, eq 12 leads to

$$\frac{1}{k_{obs} - 2k_2[I^-]^2} = \frac{k_{-1}[Fe(II)]}{2k_1k_3[I^-]^2} + \frac{1}{2k_1[I^-]} \quad (13)$$

A further simplification is achieved when the iodide concentrations are kept low:

$$\frac{1}{k_{obs}} = \frac{k_{-1}[Fe(II)]}{2k_1k_3[I^-]^2} + \frac{1}{2k_1[I^-]} \quad (14)$$

This last approximation is clearly valid for the experiments summarized in Figure 5, given the values of k_{obs} obtained, the value of k_2 listed in Table 2, and the iodide concentration employed. Equation 14 has the same form as the empirical eq 5, and thus the parameters of the linear fit to eq 5 give values of $(3.07 \pm 0.30) \times 10^6$ M^{-1} s for $k_{-1}/(2k_1k_3[I^-]^2)$ and 200 ± 8.7 s for $1/(2k_1[I^-])$ at 75 μM I^-. The ratio of these values yields 1.15 ± 0.13 for k_{-1}/k_3. The rate constant (k_3) for the association of iodide and iodine radical in acetonitrile has been reported as $(2.3 \pm 0.3) \times 10^{10}$ M^{-1} s^{-1}.[6] Accordingly, a value of $(2.4 \pm 0.5) \times 10^{10}$ M^{-1} s^{-1} is derived for k_{-1} for $[Fe(bpy)_2(CN)_2]$.

Given the large number of approximations made in deriving eq 14, a numerical test of its validity has been performed by simulating the complete proposed mechanism (eqs 6−10) using the Specfit/32 software package.[41] Note that in such simulations the rate constants are not all independent: the constraints of microscopic reversibility require that

$$\left(\frac{k_1}{k_{-1}}\right)\frac{k_3}{k_{-3}} = \frac{k_2}{k_{-2}} \quad (15)$$

Working with this constraint and using the values of k_1 and k_2 given in Table 2 and the values for k_{-1} and k_3 given above, we achieved an excellent simulation of the observed kinetic inhibition by Fe(II), as is shown in Table S-7. A full description of the simulation model is given in Table S-8.

Our derived value for k_{-1} for $[Fe(bpy)_2(CN)_2]$, $(2.4 \pm 0.5) \times 10^{10}$ M^{-1} s^{-1}, is essentially at the diffusion limit in acetonitrile. A few other reactions of uncharged species in acetonitrile have comparable rate constants, such as the reaction of $I^\bullet$ with I^- (see above) and certain reactions of $Br^\bullet$,[42] $NO_3^\bullet$,[43] and $O_2^{-\bullet}$,[44] but there appears to be none that is significantly greater. Further support for the conclusion that k_{-1} is at the diffusion limit comes from the LFER in Figure 6; moreover, this LFER implies that k_{-1} is at the diffusion limit for all four of the Fe complexes investigated in this report.

Given the values for k_1 and k_{-1} specified above for the reaction of $[Fe(bpy)_2(CN)_2]^+$, their ratio yields a value of $(1.12 \pm 0.22) \times 10^{-9}$ for K_1, the electron-transfer equilibrium constant to form the iodine atom (eq 6). This equilibrium constant implies $E_f = 0.60 \pm 0.01$ V vs $[Fe(Cp)_2]^{+/0}$ for the $I^\bullet/I^-$ redox couple if E_f for $[Fe(bpy)_2(CN)_2]^{+/0}$ is taken as the value given in Table 2.

An independent estimate of $E°$ for the $I^\bullet/I^-$ redox couple can be obtained from a thermochemical cycle involving estimates of free energies of transfer. As a starting point, it is assumed that $E° = 1.33 \pm 0.02$ V vs NHE for the aqueous $I^\bullet/I^-$ redox couple.[8] A standard potential[45] of 0.800 ± 0.001 V vs NHE for the Ag^+/Ag redox couple is then used to derive $\Delta E° = 0.53 \pm 0.02$ V or $\Delta G° = -51 \pm 2$ kJ mol^{-1} for the reaction

$$I^\bullet(aq) + Ag(s) \rightleftharpoons I^-(aq) + Ag^+(aq) \quad (16)$$

Next, the following free energies of transfer from water to acetonitrile are applied: $\Delta G°_{tr} = -23.2 \pm 2$ kJ mol^{-1} for I^-, $\Delta G°_{tr} = 16.8 \pm 2$ kJ mol^{-1} for Ag^+.[46] The approximation is made that $\Delta G°_{tr}(I^\bullet) = \Delta G°_{tr}(Xe)$, and a value of -8.4 kJ mol^{-1} is derived for this quantity from the reported Henry's law constants for Xe in water and acetonitrile.[47] These corrections lead to $\Delta G° = -49.1 \pm 3.5$ kJ mol^{-1} ($\Delta E° = 0.508 \pm 0.04$ V) for

(41) Binstead, R. A.; Jung, B.; Zuberbuhler, A. D. *Specfit/32 Global Analysis System*, version 3.0; Spectrum Software Associates: Marlborough, MA, 2000.
(42) Scaiano, J. C.; Barra, M.; Krzywinski, M.; Sinta, R.; Calabrese, G. *J. Phys. Chem.* **1993**, *115*, 8340−8344.
(43) Del Giacco, T.; Baciocchi, E.; Steenken, S. *J. Phys. Chem.* **1993**, *97*, 5451−5456.
(44) Imamura, T.; Sumiyoshi, T.; Takashi, K.; Sasaki, Y. *J. Phys. Chem.* **1993**, *97*, 7786−7791.
(45) Lingane, J. J.; Larson, W. D. *J. Am. Chem. Soc.* **1936**, *58*, 2647−2648.
(46) Marcus, Y. *Pure Appl. Chem.* **1983**, *55*, 977−1021.
(47) Brückl, N.; Kim, J. I. *Z. Phys. Chem., N. F. (Wiesbaden, Ger.)* **1981**, *126*, 133−150.

$$I^{\bullet}(AN) + Ag(s) \rightleftharpoons I^{-}(AN) + Ag^{+}(AN) \qquad (17)$$

Further corrections of 118 mV to adjust from 1 to 0.01 M Ag^+ and 0.089 V to convert from the Ag^+(0.01 M, AN)/Ag(s) reference electrode to the $[Fe(Cp)_2]^{+/0}$ reference electrode[35] finally lead to $E° = 0.54 \pm 0.04$ V for the $I^{\bullet}/I^-$ redox couple in acetonitrile vs $[Fe(Cp)_2]^{+/0}$; that is, $E°(I^{\bullet}/I^-$, AN, vs ferrocene$) = E°(I^{\bullet}/I^-$, AN, vs Ag^+/Ag, AN$) + 0.118$ V $- 0.089$ V. This result provides some support for the E_f value obtained experimentally, although there is a substantial difference between the two values.

An alternative estimate of $E°(I^{\bullet}/I^-$, AN) can be made by calculating $\Delta G°$ for reaction 17 by using the NBS values[48] for $\Delta_f G°$ of Ag^+(aq), I^-(aq), and $I^{\bullet}$(g), the $\Delta G°_{tr}$ values for Ag^+ and I^- given above, and making the approximation that the Henry's law constant for $I^{\bullet}$ in acetonitrile is the same as that of Xe. This calculation yields $\Delta G° = -56.2 \pm 3.5$ kJ mol^{-1} ($\Delta E° = 0.582 \pm 0.04$ V) for reaction 17. Correcting this to the $[Fe(Cp)_2]^{+/0}$ reference electrode then gives $E° = 0.61 \pm 0.04$ V for $I^{\bullet}/I^-$ vs $[Fe(Cp)_2]^{+/0}$ in acetonitrile. This much-improved agreement with the experimental result implies that Xe is a better model for $I^{\bullet}$ in acetonitrile than in water.

A similarly detailed analysis of k_2, the overall third-order oxidation of iodide, is not currently attainable because of uncertainties regarding the standard potential for reduction of $I_2^{-\bullet}$. Unfortunately, our observations on kinetic inhibition by Fe(II) yield data on k_{-1} but not k_{-2}. Measurements on the hemicolligation of $I^{\bullet}$ only reveal that K_{rad} in acetonitrile is at least 100-fold greater than in water.[6] This information can be combined with $E°(I^{\bullet}/I^-)$ to set an upper limit of 0.30 V vs $Fe(Cp)_2^{+/0}$ for $E°(I_2^{-\bullet}/2I^-)$. When this result is used to derive values of K_2 for the four reactions studied herein, and the values of k_2 are then used to derive values for k_{-2}, none are greater than 2.2×10^8 M^{-1} s^{-1}. Thus, all of the reactions have k_{-2} values that are well below the diffusion limit, which is in agreement with the conclusion derived from the slope of the LFER for k_2 in Figure 6.

Direct measurements of the rate of reduction of Fe(III) complexes by iodide in dye-sensitized solar cells appear not to have been reported. From the present results, it would be reasonable to anticipate that copper catalysis could be significant. In the presence of potential inhibitors such as the pyridines often present in the electrolyte, one could anticipate a rate law for the heterogeneous reaction with terms first-order and second-order in $[I^-]$ as has been previously suggested for Ru- and Os-based sensitizers.[49] The individual rate constants would be anticipated to depend on $E°$ of the sensitizer as given by the slopes of the LFERs in Figure 6. Our reported value for $E°(I^{\bullet}/I^-)$ can provide a rigorous test of rate constants for the first-order oxidation of I^- by adsorbed dyes, since the reverse rate constants must not exceed the diffusion-controlled limit. The LFER for k_1 provides a method for the quantitative prediction of rate constants for reduction of adsorbed sensitizers that are first-order in $[I^-]$, since the reverse paths are predicted to have diffusion-controlled rate constants. This predictive capability should be of value, given the report that iodide oxidation can be the limiting factor in certain dye-sensitized solar cells.[49]

Conclusions. Trace copper-ion catalysis appears to be a general phenomenon in oxidations of iodide by outer-sphere oxidants in acetonitrile. When this catalysis is thoroughly inhibited, the direct oxidation of iodide has the same stoichiometry and two-term rate law as in aqueous solutions. A further parallel with the aqueous chemistry is that the rate constants conform to LFERs that imply the reverse rate constants for the two paths are diffusion-controlled and activation controlled, respectively. The intermediacy of $I^{\bullet}$ and $I_2^{-\bullet}$ is inferred, and the standard potential for the $I^{\bullet}/I^-$ redox couple is derived from the kinetic inhibition by Fe(II).

Acknowledgment. The authors thank Professors Lewis, Gray, and Anson (California Institute of Technology) for initially suggesting this project and the National Science Foundation (NSF) for funding this research. This material is based on work supported by the NSF under Grant Nos. 0138142 and 0509889. Any opinions, findings, conclusions, or recommendations expressed in this material are those of the author(s) and do not necessarily reflect the views of the NSF.

Supporting Information Available: Tables S-1 to S-8, Figures S-1 to S-7, details on the kinetic effects of water, and a derivation of eq 11. This material is available free of charge via the Internet at http://pubs.acs.org.

IC052022Y

(48) Wagman, D. D.; Evans, W. H.; Parker, V. B.; Schumm, R. H.; Halow, I.; Bailey, S. M.; Churney, K. L.; Nuttall, R. L. *J. Phys. Chem. Ref. Data* **1982**, *11* (Suppl. 2).

(49) Alebbi, M.; Bignozzi, C. A.; Helmer, T. A.; Hasselmann, G. M.; Meyer, G. J. *J. Phys. Chem. B* **1998**, *102*, 7577−7581.